

Chapter 9. Deterministic Chaos

This chapter gives a brief review of chaotic phenomena in maps and dynamic systems with and without dissipation, and a very short discussion of the possible role of chaos in fluid turbulence.

9.1. Chaos in maps

Chaotic behavior of dynamic systems (sometimes called the *deterministic chaos*) was theoretically discovered¹ in 1963 by E. Lorenz who was examining numerical solutions of a system of three nonlinear, ordinary differential equations of the first order:

$$\begin{aligned}\dot{q}_1 &= a_1(q_2 - q_1), \\ \dot{q}_2 &= a_2q_1 - q_2 - q_1q_3, \\ \dot{q}_3 &= q_1q_2 - a_3q_3.\end{aligned}\tag{9.1}$$

as a rudimentary model for heat transfer through a horizontal layer of fluid between two solid plates. (Experiment shows that if the lower plate is kept hotter than the top one, this system may exhibit turbulent convection.) He has found that within a certain range of constants $a_{1,2,3}$, the solutions follow complex, unpredictable, non-repeating trajectories in the q -space. In another language, the resulting functions $\{q_1(t), q_2(t), q_3(t)\}$ are so sensitive to initial conditions $\{q_1(0), q_2(0), q_3(0)\}$, that at sufficiently large times t , solutions corresponding to slightly different initial conditions are completely different.

Very soon it was realized that such behavior is typical for even simpler mathematical objects called *maps*, so that I will start my discussion of chaos from these objects. A 1D map is essentially a rule for finding the next number q_{n+1} of a series, in the simplest case using only its last known value q_n . The most famous example is the so-called *logistic map*:²

$$q_{n+1} = f(q_n) \equiv rq_n(1 - q_n).\tag{9.2}$$

The basic properties of this map may be understood using the (hopefully, self-explanatory) graphical presentation shown in Fig. 1.³ One can readily see that at $r < 1$ the map rapidly converges to fixed point $q^{(0)} = 0$, because each next value of q is less than the previous one. However, if r is increased above 1 (like in the example shown in Fig. 1), fixed point $q^{(0)}$ becomes unstable. Indeed, at $q_n \ll 1$, map (2) yields $q_{n+1} = rq_n$, so that at $r > 1$, q_n grow with each iteration. Instead of that unstable point, in the range $1 < r < r_1$, where $r_1 \equiv 3$, the map has a stable point, $q^{(1)}$, which may be found by plugging this value into both parts of Eq. (2):

$$q^{(1)} = rq^{(1)}(1 - q^{(1)}),\tag{9.3}$$

giving $q^{(1)} = (1 - 1/r)$ – see the left branch in Fig. 2.

¹ Actually, the notion of quasi-random dynamics due to the exponential divergence of trajectories may be traced back at least to (apparently independent) works by A. Poincaré in 1892 and by J. Hadamard in 1898.

² It was first discussed in detail in 1976 by R. May, on the basis of simple demographic models considered as early as in 1838 by P. Verhulst.

³ Since the maximum value of function $f(q)$, achieved at $q = 1/2$, equals $r/4$, the mapping may be limited by segment $x = [0, 1]$ only if parameter r is between 0 and 4. Since all interesting properties of the map, including chaos, may be found within these limits, I will focus on this range.

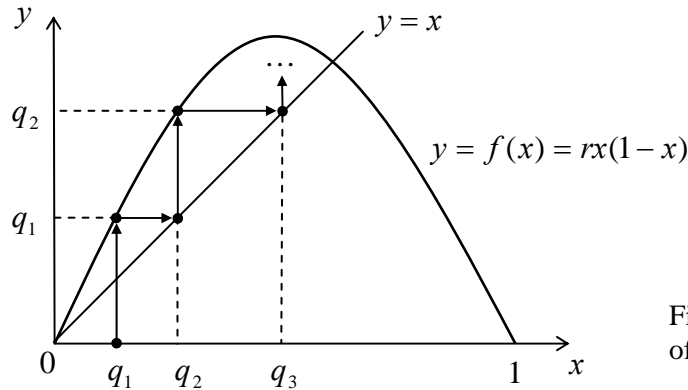


Fig. 9.1. Graphical analysis of the logistic map.

At $r > r_1$, the plot gets thicker: here the fixed point $q^{(1)}$ also becomes unstable. To prove that, let us take $q_n = q^{(1)} + \tilde{q}_n$, assume that deviation \tilde{q}_n from the fixed point $q^{(1)}$ is small, and linearize map (3) in \tilde{q}_n , just as we repeatedly did for differential equations earlier in this course. The result is

$$\tilde{q}_{n+1} = \left. \frac{df}{dq} \right|_{x=q^{(1)}} \tilde{q}_n = r(1 - 2q^{(1)})\tilde{q}_n = (2 - r)\tilde{q}_n. \tag{9.4}$$

It shows that $(2 - r) > 0$, i.e. $r < 2$, deviations \tilde{q}_n decrease monotonically. At $0 < (2 - r) < -1$, i.e. $2 < r < 3$, they their signs alternate but the magnitude still decreases (as in a stable focus). However, at $(2 - r) < -1$, i.e. $r > r_1 = 3$, the deviations are growing by magnitude, while still changing sign, at each step. Since Eq. (2) has no other fixed points, this means that at $n \rightarrow \infty$, values q_n do not converge; rather, within the range $r_1 < r < r_2$, they approach the *limit cycle* of alternation between two points, $q_+^{(2)}$ and $q_-^{(2)}$ which satisfy the following system of algebraic equations

$$q_+^{(2)} = f(q_-^{(2)}), \quad q_-^{(2)} = f(q_+^{(2)}). \tag{9.5}$$

(These points are also plotted in Fig. 2.) What has happened in point r_1 is called the *period-doubling bifurcation*. The story repeats at $r = r_2 = 1 + \sqrt{6} \approx 3.45$ where the system goes from the 2-point limit cycle to a 4-point cycle, then at point $r = r_3 \approx 3.54$ at which the limit cycle gets 8 alternating points, etc.

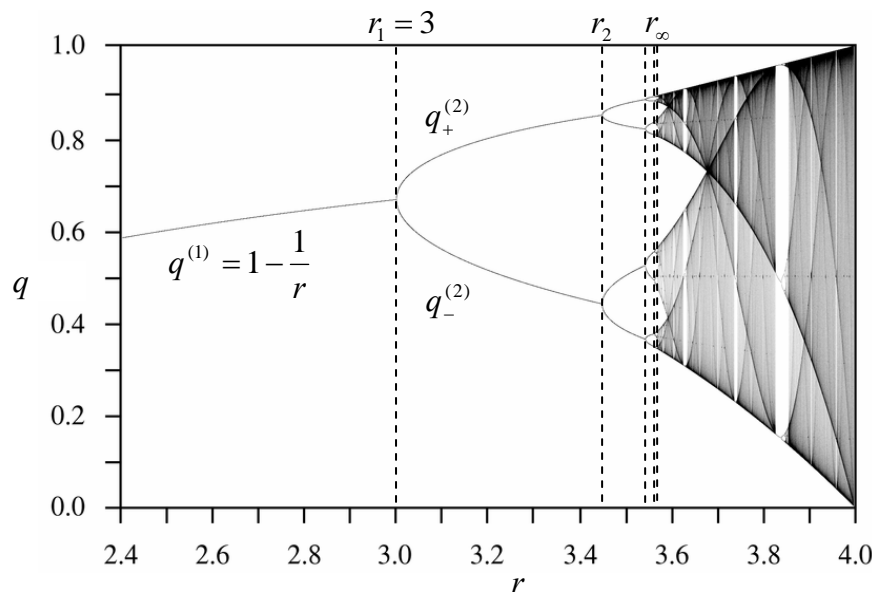


Fig. 9.2. Fixed points and chaotic regions of the logistic map. Plot adapted from http://en.wikipedia.org/wiki/Logistic_map; a very nice live simulation of the map is also available at that Web site.

Most remarkably, the period-doubling bifurcation points r_n , at which the number of points in the limit cycle doubles from 2^{n-1} points to 2^n points, become closer and closer. Numerical calculations have shown that these points obey the following asymptotic behavior:

$$r_n \rightarrow r_\infty - \frac{C}{\delta^n}, \quad r_\infty = 3.5699\dots, \quad \delta = 4.6692\dots \quad (9.5)$$

Actually, parameter δ , called the *Feigenbaum constant*, has been by now calculated to more than 1,000 decimal places! (Just as in the case of number π , this is not much more than a demonstration of the computation muscle.) For other maps, and some dynamic systems (see the next section), the period-doubling sequence follows a similar law, but with different parameters C and δ .

More important for us, however, is what happens at $r > r_\infty$. Numerous numerical experiments, repeated with increasing precision,⁴ have confirmed that here the system is fully disordered, with no reproducible limit cycle, though (as Fig. 2 shows) at $r \approx r_\infty$, all sequential values q_n are still confined to a few narrow regions.⁵ However, as parameter r is increased well beyond r_∞ , these regions broaden and merge. This is the so-called *full*, or *well-developed* chaos, with no apparent order at all.⁶

The most important feature of chaos (in this and any other system) is the *exponential divergence of trajectories*. For a 1D map, this means that even if initial conditions x_1 in two map implementations differ by a very small amount Δx_1 , the difference Δx_n between the corresponding sequences x_n is growing (on the average) exponentially with n . Moreover, such exponents may be used to characterize chaos. Indeed, let us consider a simple case when all values q_n , starting from some number $n = n_0$, be sufficiently close to each other. Then an evident generalization of the first of Eqs. (4) to an arbitrary point yields

$$|\tilde{q}_{n+1}| = |f'_n| |\tilde{q}_n|, \quad f'_n \equiv \left. \frac{df}{dq} \right|_{q=q_n}. \quad (9.6)$$

Using this result iteratively for N steps, we get

$$|\tilde{q}_{n_0+N}| = |\tilde{q}_{n_0}| \prod_{n=n_0}^{n_0+N} |f'_n|, \quad (9.7)$$

to that

$$\ln \left| \frac{\tilde{q}_{n_0+N}}{\tilde{q}_{n_0}} \right| = \sum_{n=n_0}^{n_0+N} \ln |f'_n|. \quad (9.8)$$

⁴ The reader should remember that just as the usual (“nature”) experiments, numerical experiments also have limited accuracy, due to unavoidable rounding errors.

⁵ The geometry of these regions are essentially *fractal*, i.e. has a dimensionality intermediate between zero (which any final set of geometric points would have) and one (pertinent to a 1D continuum). A deep discussion of fractal geometries, and their relation to the deterministic chaos may be found, e.g., in the book by B. B. Mandelbrot, *The Fractal Geometry of Nature*, W. H. Freeman, 1983.

⁶ This does not mean that the chaos development is a monotonic function of r . As Fig. 2 shows, within certain intervals of this parameter chaos suddenly disappears, being replaced, typically, with a few-point limit cycle, just to resume on the other side of the interval. Sometimes (but not always!) the “route to chaos” on the borders of these intervals follows the same Feigenbaum sequence of period-doubling bifurcations.

Numerical experiments show that in most chaotic regimes, at $N \rightarrow \infty$ this sum fluctuates about an average value which grows as λN , with parameter

$$\lambda = \lim_{N \rightarrow \infty} \frac{1}{N} \sum_{n=n_0}^{n_0+N} \ln |f'_n|. \quad (9.9)$$

(called the *Lyapunov exponent*),⁷ independent on the initial conditions and N_0 (if $N_0 \gg 1$).⁸ Hence, the Lyapunov exponent may be used for map characterization; the bottom panel in Fig. 3 shows it as a function of the parameter r for the logistic map. Note that at $r < r_\infty$, λ is negative, indicating the trajectory stability, besides points r_1, r_2, \dots where λ would become positive in the limit cycle change had not brought it back to the negative territory. However, at $r > r_\infty$, λ becomes positive, returning the negative values only in the limited intervals of finite limit cycle stability. It is evident that in numerical experiments (which dominate the studies of chaos) the Lyapunov exponent may be used as a good measure of the “depth” of chaos.⁹

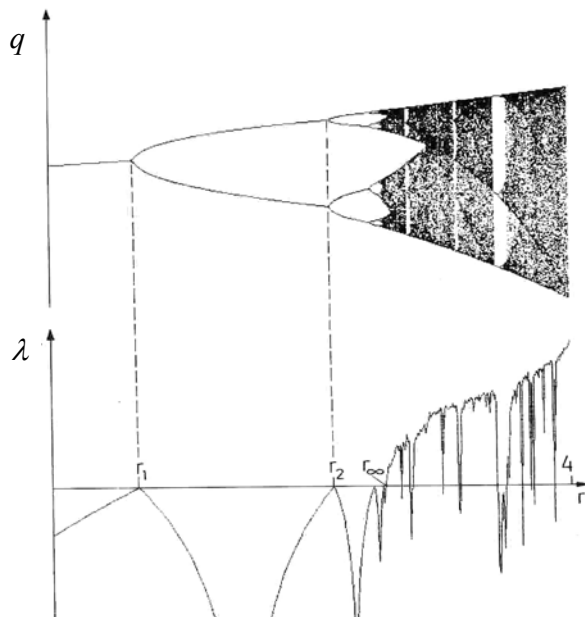


Fig. 9.3. The Lyapunov exponent for the logistic map. Adapted from the book by Schuster and Just (cited below).

Despite all the abundance of results for particular maps,¹⁰ it is important to emphasize that despite several interesting general results (like the Feigenbaum bifurcation sequence), nobody knows yet how to predict the patterns like those shown in Fig. 2 and 3, from just looking at the map itself, i.e.

⁷ After A. Lyapunov (1857-1918), famous for his studies of stability of dynamic systems.

⁸ If the values q_n are not close to each other, Eq. (6) is not strictly valid, and Eq. (9) has to be generalized, but the very notion of the Lyapunov exponent is still valid.

⁹ N -dimensions maps, which relate N -dimensional vectors rather than scalars, may be characterized by N Lyapunov exponents rather than one. In order to reach chaos, it is sufficient for just of them to become positive. For such systems, another measure of chaos, the *Kolmogorov entropy*, may be more relevant. This measure, and its relation with the Lyapunov exponents, will be discussed in the Statistical Mechanics part of my course series.

¹⁰ See, e.g., Chapters 2-4 in H. G. Schuster and W. Just, *Deterministic Chaos*, 4th ed., Wiley-VCH, 2005, or Chapters 8-9 in J. M. T. Thompson and H. B. Stewart, *Nonlinear Dynamics and Chaos*, 2nd ed., Wiley, 2002.

without carrying out actual numerical experiments with in. Unfortunately the situation with chaos in other systems is not much better.

9.2. Chaos in dynamic systems

Proceeding to chaos in systems described by systems of ordinary differential equations, with our background, it is more natural to use for this purpose not the original system (1), but equations describing a dissipative pendulum driven by a sinusoidal external force, which was repeatedly discussed in Chapter 3. Introducing two new variables, the normalized momentum $p \equiv (dq/dt)/\omega_0$ and the external force's full phase $\psi \equiv \omega t$, we may rewrite Eq. (4.42) describing the pendulum,

$$\ddot{q} + 2\delta\dot{q} + \omega_0^2 \sin q = f_0 \cos \omega t, \quad (9.10)$$

in a form similar to Eq. (1), i.e. as a system of three first-order differential equations:

$$\dot{q} = \omega_0 p, \quad \dot{p} = -\omega_0 \sin q - 2\delta p + (f_0 / \omega_0) \cos \psi, \quad \dot{\psi} = \omega. \quad (9.11)$$

Figure 4 several results of numerical solution of Eq. (9).¹¹ In all cases, the internal parameters δ and ω_0 of the system, and the external force amplitude f_0 are the same, while the external frequency ω is gradually changed. For the case shown in the top frame, the system still tends to a stable periodic solution, with low contents of higher harmonics. If the external force frequency is reduced by a just few percent, the 3rd subharmonic may be excited. (This effect has already been discussed in Sec. 4.7.) The next panel shows that just a very small further reduction of frequency leads to a new tripling of the period, i.e. the generation of a complex waveform with 9th subharmonic. Finally, even a minor further change of parameters leads to oscillations without any visible period, e.g. chaos.

In order to trace this transition, direct observation of the oscillation waveforms $x(t)$ is not very useful, and trajectories on the phase plane $[q, p]$ also become messy if plotted for many periods of the external frequency. In situations like this, the Poincaré (or “stroboscopic”) plane, already discussed in Sec. 4.6, is much more useful. As a reminder, this is essentially just the phase plane $[q, p]$, but with the points highlighted only once a period, e.g., at $\psi = 2\pi n$, $n = 1, 2, \dots$ ¹² On this plane, a periodic oscillation of frequency ω is presented just as one fixed point – see, e.g. the top panel in the right column of Fig. 4. The beginning of the 3rd subharmonic generation means tripling of the oscillation period, and is reflected on the Poincaré plane by splitting the fixed point into three. It is evident that this transition may be paralleled with the period-doubling bifurcation in the logistic map.¹³ From this point, the 9th harmonic generation, i.e. one more splitting of the points on the Poincaré plane, may be understood as one more step on the Feigenbaum-like route to chaos.

¹¹ In the actual simulation, a small term εq , with $\varepsilon \ll 1$, has been added to the left-hand part of this equation. This term slightly somewhat tames the trend of the solution to spread along q axis, and makes the presentation of results easier, without affecting the system dynamics too much.

¹² As one more reminder, in the case when the waveform may be presented (as it is assumed, e.g., in the van der Pol method which was discussed in Sec. 4.3) as a sinusoidal oscillation with slowly changing amplitude and phase, $q(t) \approx A(t)\cos[\omega t - \varphi(t)] = u(t)\cos\omega t + v(t)\sin\omega t$, the Poincaré plane is just the phase plane of the van der Pol variables, with Cartesian coordinates $[u, v]$ and polar coordinates $[A, \varphi]$.

¹³ The 2nd subharmonic generation, e.g., the period doubling, in the pendulum is suppressed by the symmetry of its nonlinearity. In systems of equations which lack such symmetry, the Feigenbaum period-doubling sequence is a more frequent (though not the universal) route to chaos.

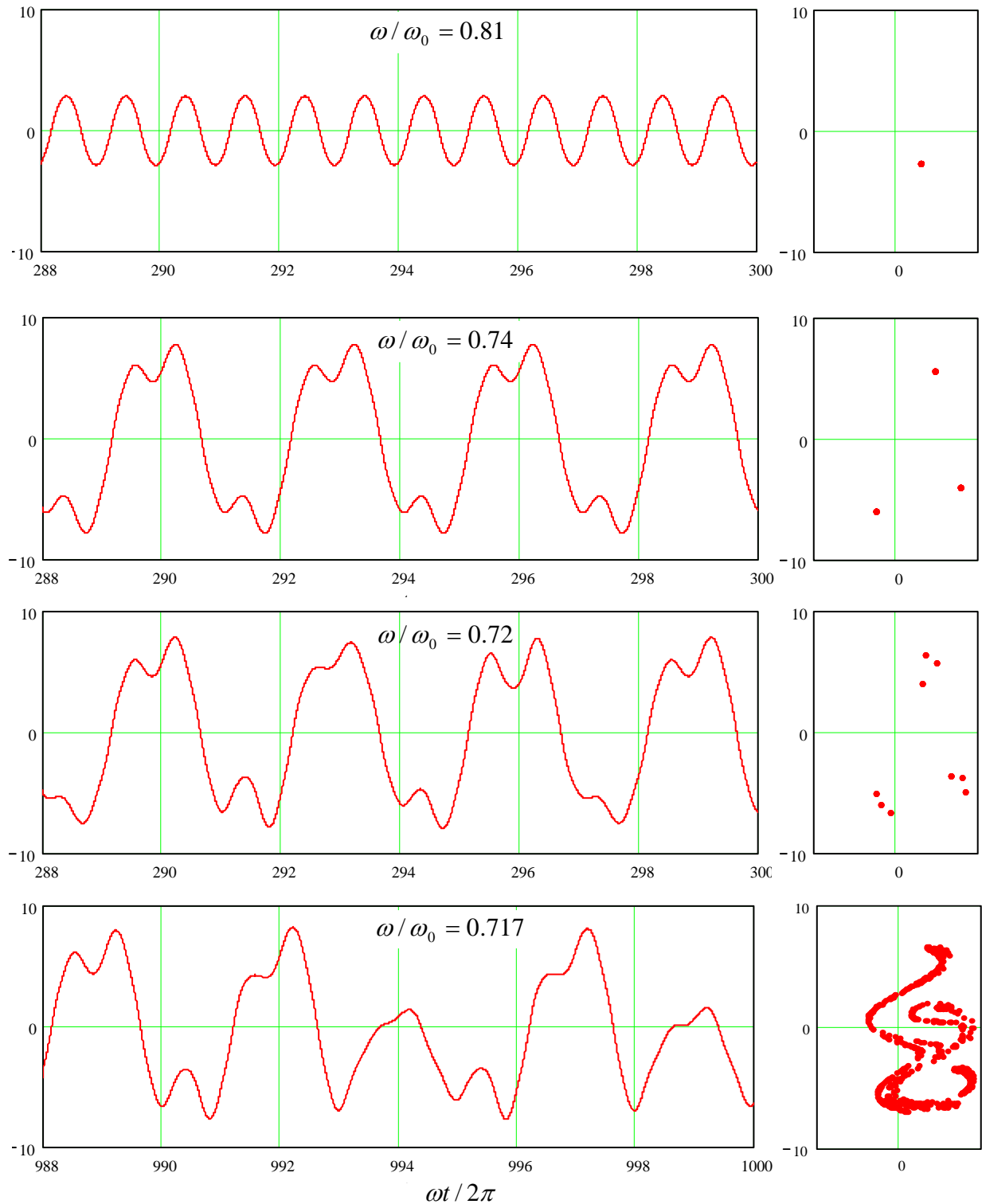


Fig. 9.4. Oscillations in a pendulum with weak damping, $\delta/\omega_0 = 0.1$, driven by a sinusoidal external force with amplitude $f_0/\omega_0^2 = 1$ and several close frequencies (listed on the panels). Left column: oscillation waveforms $q(t)$ recorded after certain initial transient periods. Right column: presentation of the same processes on a the Poincaré plane of variables $[p, q]$.

So, the transition to chaos in dynamic systems may be at least qualitatively similar to than in 1D maps, with the similar law (5) for the critical values of the system parameter, though generally with a different value of the Feigenbaum exponent δ . Moreover, it is evident that we can always consider the first two differential equations of system (11) as a 2D map which relates the vector $\{q_{n+1}, p_{n+1}\}$ of the coordinate and velocity, measured at $\psi = 2\pi(n + 1)$, to the previous value $\{q_n, p_n\}$ of that vector (reached at $\psi = 2\pi n$). Unfortunately this similarity also implies that chaos in *dynamical systems* (the term understood usually as “systems described by deterministic differential equations”) is at least as complex, and it as little understood, as in maps.

For example, Fig. 5 shows (a part of) the state diagram of the externally-driven pendulum, with the red bar marking the route to chaos traced in Fig. 4, and different shading marking different regimes. One can that the pattern is at least as complex as that shown in Figs. 2, 3 and, besides a few features,¹⁴ equally unpredictable from the form of the equation.

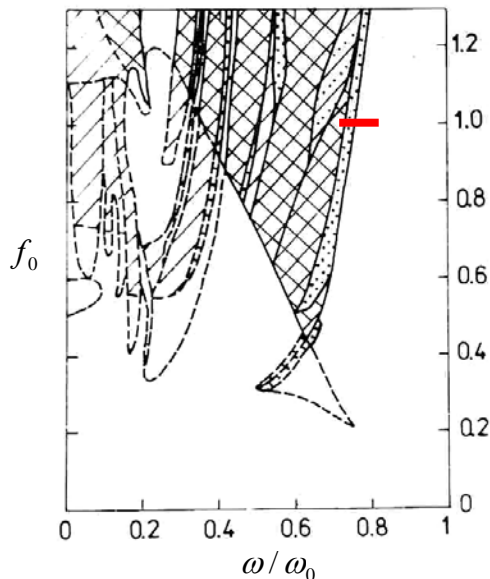


Fig. 9.5. Phase diagram of an externally-driven pendulum with $\delta/\omega_0 = 0.1$. Regions of oscillations with the basic period are not shaded. The notation for other regions is as follows. Doted: subharmonic generation; cross-hatched: chaos; hatched: chaos or basic period (depending on the initial conditions); hatch-dotted: basic period or subharmonics. Solid lines show boundaries of single-regime regions, while dashed lines are boundaries of regions in which several types of motion are possible, depending on history. Adapted from V. K. Kornev and V. K. Semenov, *IEEE Trans. on Magn.* **19**, 633 (1983).

Are there any valuable general results concerning chaos in the dynamical systems? The most important (though almost evident) result is that this phenomenon is impossible in any system described by one or two first-order differential equations with right-hand parts independent of time. Indeed, let us start with a single equation

$$\dot{q} = f(q), \quad (9.12)$$

where $f(x)$ is a usual single-valued function. This equation may be directly integrated (just as was made with the first integrals of motion in Sec. 3.3):

¹⁴ For example, frequently one can predict a parameter region where chaos *cannot* happen, due to lack of instability-amplification mechanism. Unfortunately, typically the boundaries of such region do not form a very tight envelope of the actual chaotic regions. In other words, in many cases, chaos does not materialize even when it apparently may take place.

$$t = \int^q \frac{dq'}{f(q')} + \text{const}, \quad (9.13)$$

so that the relation between q and t is unique and does not leave place for chaos.

Now, let us explore the system of two equations:

$$\begin{aligned} \dot{q}_1 &= f_1(q_1, q_2), \\ \dot{q}_2 &= f_2(q_1, q_2). \end{aligned} \quad (9.14)$$

Consider its phase plane shown schematically in Fig. 6. In a “usual” system, the trajectories approach either some fixed point (Fig. 6a) describing equilibrium, or a limit cycle (Fig. 6b) describing periodic oscillations. (Both notions are united by the term *attractor*, because they “attract” trajectories launched from various initial positions.) However, phase plane trajectories in a chaotic system equations, which describe real physical variables (which cannot tent to infinity), should be confined to limited phase area, and simultaneously cannot start repeating each other. (This topology is frequently called “*strange attractor*”.) For that, 2D trajectories need to cross – see, e.g., point A in Fig. 6c.

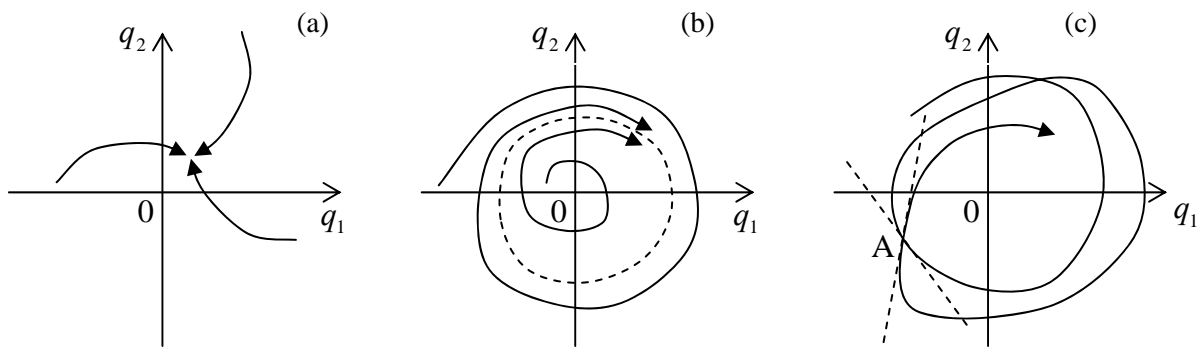


Fig. 9.6. Types of attractors in dynamical systems: (a) fixed point, (b) limit cycle, and (c) strange attractor.

However, in the case (14) this is clearly impossible, because according to these equations the tangent slope is a unique function of point $\{q_1, q_2\}$ on the phase plane:

$$\frac{dq_1}{dq_2} = \frac{f_1(q_1, q_2)}{f_2(q_1, q_2)}. \quad (9.15)$$

We see that in this case chaos is impossible. It becomes, however, readily possible, if the right-hand parts of a system similar to Eq. (14) depends either on other variables of the system or time. For example, if we consider the first two differential equations of system (11), in the case $f_0 = 0$ they have the structure of the system (14) and hence chaos is impossible, even at with $\delta < 0$ when (as we know from Sec. 4.4) the system allows self-excitation of oscillations. However, if $f_0 \neq 0$, this argument does not work any longer and (as we have already seen) the system may have a strange attractor – which is, for dynamic system, a synonym to the deterministic chaos. Thus, chaos is possible in dynamic systems which may be described by three or more differential equations of the first order.¹⁵

¹⁵ Since a typical dynamic system with one degree of freedom is described by two such equations (see Footnote 22 in Ch. 4), the number of first-order equations is sometimes called the number of “*half-degrees of freedom*”.

9.3. Chaos in Hamiltonian systems

The last analysis is of course valid for Hamiltonian systems, which are just a particular type of dynamical systems. However one may wonder whether these systems, which feature at least one first integral of motion, $H = \text{const}$, and hence are more “ordered” than the systems discussed above, can exhibit chaos at all. The question is yes, because such systems can still provide mechanisms for an exponential growth of a small initial perturbation.

As the simplest way to show it, let us consider a so-called *mathematical billiard*, i.e. a ballistic particle (a “ball”) moving freely on a horizontal plane surface (“table”) limited by walls. In this idealized model of the usual game of billiards, ball’s velocity \mathbf{v} is conserved when it moves on the table, and when it runs into a table’s wall, the ball is elastically reflected from it as from a mirror,¹⁶ with the reversal of the sign of the normal velocity v_n , and conservation of the tangential velocity v_τ , and hence without any loss of its kinetic (and hence the full) energy,

$$E = H = T = \frac{m}{2} v^2 = \frac{m}{2} (v_n^2 + v_\tau^2). \quad (9.16)$$

This model, while being a legitimate 2D dynamic system,¹⁷ allows geometric analyses for several simple table shapes. The simplest case is a rectangular billiard of area $a \times b$ (Fig. 7), whose analysis may be readily carried out by the replacement of each *ball* reflection event with the mirror reflection of the *table* in that wall – see dashes lines in panel (a).

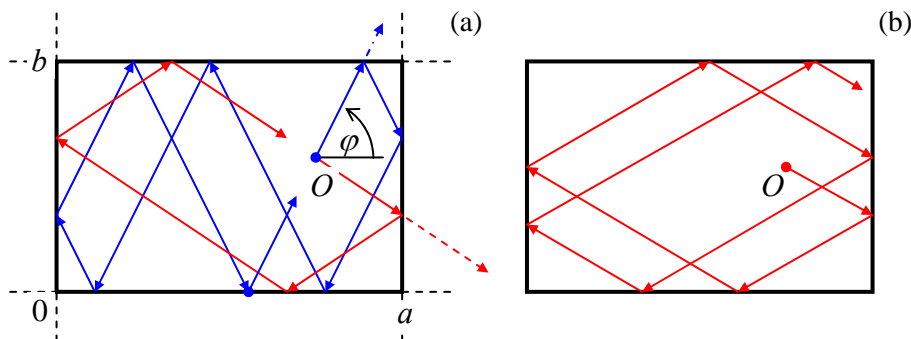


Fig. 9.7. Ball motion on a rectangular billiard at (a) commensurate and (b) incommensurate launch angle.

Such analysis (left for reader’s pleasure:-) shows that if the tangent of the ball launching angle φ is commensurate with the side length ratio,

$$\tan \varphi = \pm \frac{m}{n} \frac{b}{a}, \quad (9.17)$$

where n and m are non-negative integers without common integer multipliers, the ball returns exactly to the launch point O , after bouncing m times from each wall of length a , and n times from each wall of length b . (Red lines in Fig. 7a show an example of such trajectory for $n = m = 1$, while blue lines, for $m = 3, n = 1$.) Thus the larger is the sum $(m + n)$, the more complex is such closed trajectory (“orbit”).

¹⁶ A more scientific-sounding name for such reflection is “*specular*” (from “*speculum*”, an rarely used word meaning a metallic mirror).

¹⁷ Indeed, it is fully described by Lagrangian $L = mv^2/2 - U(\mathbf{r})$, with $U(\mathbf{r}) = 0$ for 2D vectors \mathbf{r} belonging to the table area, and $U(\mathbf{r}) = +\infty$ outside of the area – cf. Problem 3.2.

Finally, if $(n + m) \rightarrow \infty$, i.e. $\tan\varphi$ and b/a are incommensurate (their ratio is an irrational number), the trajectory covers all the table area, and the ball never returns exactly into the launch point. Still, this is not chaos. Indeed, a small shift of the launch point shifts all the trajectory fragments by the same displacement. Moreover, at any time t , each of Cartesian components $v_j(t)$ of the ball's velocity (with coordinate axes parallel to the table sides) may take only two values, $\pm v_j(0)$, and hence vary as much as the initial velocity is being changed.

In 1963, Ya. Sinai showed that the situation changes completely if an additional wall, in the shape of a circle, is inserted into a rectangular billiard (Fig. 8). For most initial conditions, ball's trajectory eventually runs into the circle (see the red line on panel (a) as an example), and the further trajectory becomes essentially chaotic. Indeed, let us consider the ball's reflection from the circle-shaped wall – Fig. 8b. Due to the conservation of the tangential velocity, and sign change of the normal velocity component, the reflection obeys the mechanical analog of the Snell law (cf. Fig. 7.12 and its discussion): $\theta_r = \theta_i$. Figure 8b shows that as the result, a small difference $\delta\varphi$ between the angles of two close trajectories (as measured in the lab system), doubles by magnitude at each reflection from the curved wall. This means that the small deviation grows along the ball trajectory as

$$|\delta\varphi(N)| = |\delta\varphi(0)| \times 2^N = |\delta\varphi(0)| e^{N \ln 2}, \quad (9.18)$$

where N is the number of reflections from the convex wall.¹⁸ As we already know, such exponential divergence of trajectories, with a positive Lyapunov exponent, is the sign of deterministic chaos.¹⁹

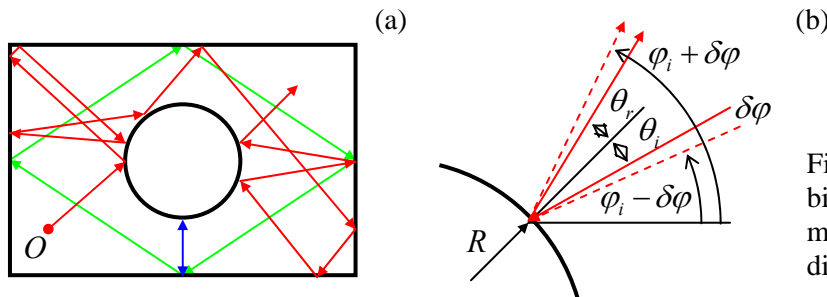


Fig. 9.8. (a) Motion on a Sinai billiard table, and (b) the mechanism of the exponential divergence of close trajectories.

Perhaps, the most important new feature of the chaos in Hamiltonian systems is its dependence on initial conditions. (In the systems discussed in two previous sections, which lack the first integrals of motion, the initial conditions are rapidly “forgotten”.) Indeed, even a Sinai billiard allows periodic motion, along closed orbits, at certain initial conditions – see blue and green lines in Fig. 8a as examples. Thus the chaos “depth” in such systems may be characterized by the fraction²⁰ of the phase

¹⁸ Actually, concave walls may also make a billiard chaotic. A famous example is the “stadium” billiard, suggested by L. Bunimovich, with two straight, parallel walls connecting two semi-circular, concave walls. Another example, which allows a straightforward analysis, is the *Hadamard billiard*, an infinite (or rectangular) table with non-horizontal surface of negative curvature.

¹⁹ Billiards are also a convenient platform for a discussion of a conceptually important issue of quantum properties of classically chaotic systems (sometimes misnamed as “quantum chaos”) – see, e.g., QM Ch. 4.

²⁰ Actually, quantitative characterization of the fraction is not trivial, because it may have fractal dimensionality. Unfortunately, due to lack of time I have to refer the reader interested in this issue to special literature, e.g., the monograph by B. B. Mandelbrot, which was cited above, and references therein.

space of initial parameters (for a 2D billiard, the 3D space of initial values of x , y , and φ) resulting in chaotic trajectories.

This conclusion is also valid for Hamiltonian systems which are met in experiments more frequently than the billiards, for example, coupled nonlinear oscillators without damping. Probably, the most popular example is the so-called *Hénon-Heiles* system,²¹ which may be described by the following Lagrangian function:

$$L = \frac{m_1}{2}(\dot{q}_1^2 - \omega_1^2 q_1) + \frac{m_2}{2}(\dot{q}_2^2 - \omega_2^2 q_2) - \varepsilon \left(q_1^2 - \frac{1}{3} q_2^2 \right) q_2. \quad (9.19)$$

(Most studies of this equation have been carried out for the following particular case: $m_2 = 2m_1$, $m_1\omega_1^2 = m_2\omega_2^2$. In this case, introducing new variables $x \equiv \varepsilon^{1/3} q_1$, $y \equiv \varepsilon^{1/3} q_2$, and $\tau \equiv \omega_1 t$, it is possible to rewrite Eq. (19) in parameter-free form. All the results shown below (Fig. 20) are for this case.) It is straightforward to use Eq. (19) to derive the Lagrangian equations of motion,

$$m_1(\ddot{q}_1 + \omega_1^2 q_1) = -2\varepsilon q_1 q_2, \quad m_2(\ddot{q}_2 + \omega_2^2 q_2) = -\varepsilon(q_1^2 - q_2^2), \quad (9.20)$$

and find its first integral of motion (physically the energy conservation law):

$$H = E = \frac{m_1}{2}(\dot{q}_1^2 + \omega_1^2 q_1) + \frac{m_2}{2}(\dot{q}_2^2 + \omega_2^2 q_2) + \varepsilon \left(q_1^2 - \frac{1}{3} q_2^2 \right) q_2 = \text{const}. \quad (9.21)$$

In the context of our discussions in Chapter 4 and 5, Eq. (20) may be readily interpreted as an equation of two oscillators, with small-oscillation eigenfrequencies ω_1 and ω_2 , coupled only by nonlinear terms in the right-hand parts of the differential equations. This means that as the oscillation amplitudes $A_{1,2}$, and hence the total energy E of the system, tend to zero, the oscillator subsystems are virtually independent, each performing sinusoidal oscillations at its own frequency.

This observation suggests a convenient way to depict the system motion. (Generally, it is a trajectory in 4D space, e.g., that of coordinates $q_{1,2}$ and their time derivatives, though the first integral of motion (21) means that for each fixed energy E , the motion is limited to a 3D sub-space. Still, this is too much for convenient presentation of results.) Let us consider a Poincaré plane for one of the oscillators (say, q_2), similar to that discussed in Sec. 2 above, with the only difference is that (because of the absence of an explicit function of time, like that in Eq. (10)), the trajectory on the $[q_2, \dot{q}_2]$ plane is highlighted at the moments when $q_1 = 0$.

Let us start from the limit $A_{1,2} \rightarrow 0$, when oscillations of q_2 are virtually sinusoidal. As we already know (see Fig. 4.9 and its discussion), if the point highlighting was perfectly synchronous with frequency ω_2 of the oscillations, there would be only one point on the Poincaré plane – see, e.g. the right top plane in Fig. 4. However, at q_1 – initiated highlighting, there is not such synchronism, so that each period a different point of the elliptical (at the proper scaling of the velocity, circular) trajectory is highlighted, so that the resulting points, for certain initial conditions, reside on a circle of radius A_2 . If we now vary the initial conditions, but keep the total energy E constant, on the Poincaré plane we get a series of circles, each pertaining to the specific distribution of the initial energy between the two oscillators.

²¹ First studied in 1964 by M. Hénon and C. Heiles as a simple model of star rotation about a galactic center.

Now, if the initial energy is increased, nonlinear interaction of the oscillations start to deform these circles, causing also their crossings – see, e.g., the top left panel of Fig. 9. Still, to a certain limit, all Poincaré points belonging to a certain initial condition, sit on a single closed contour. Moreover, these contours may be calculated approximately, but with a pretty good accuracy, using a straightforward generalization of the small parameter method discussed in Sec. 4.2.²²

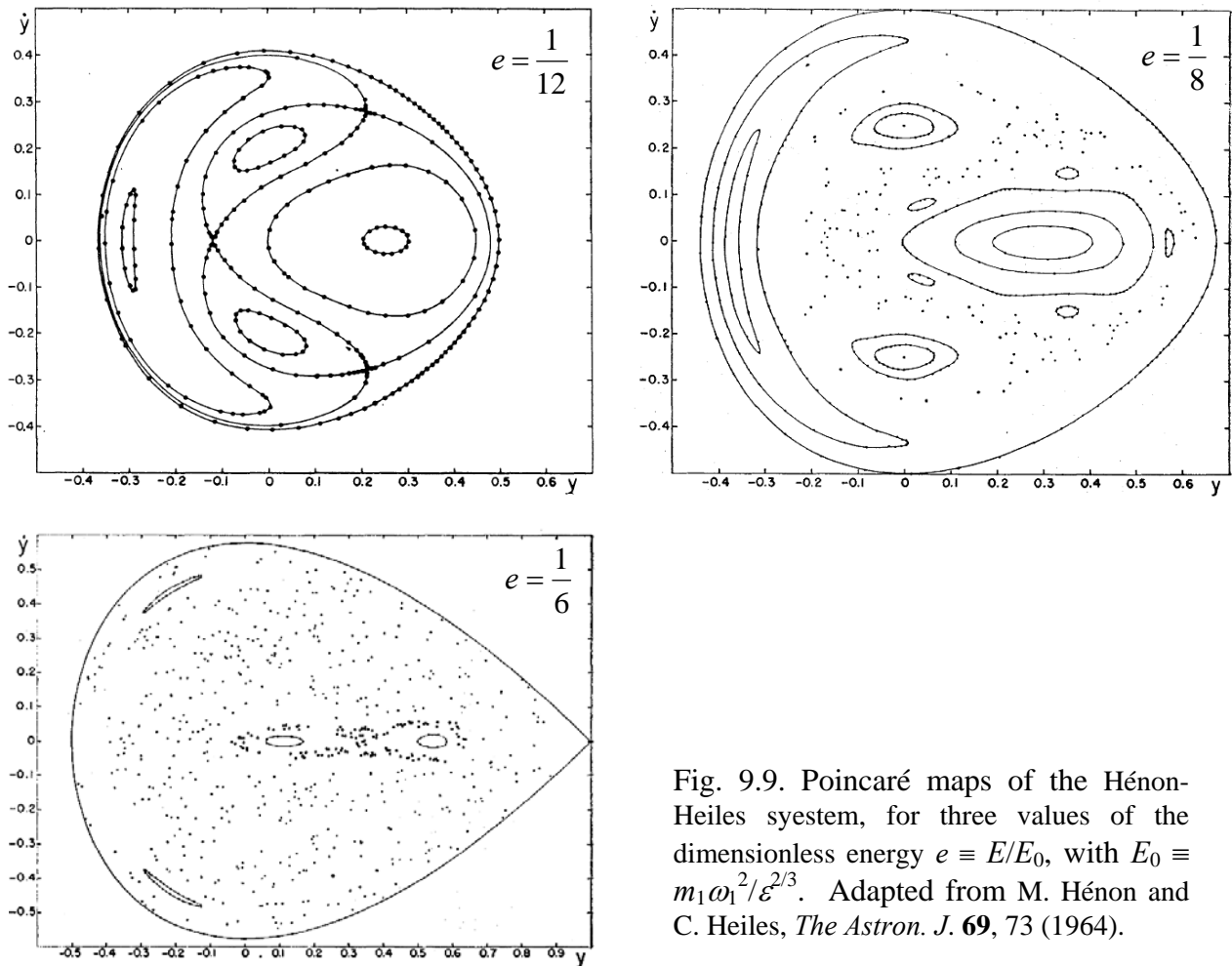


Fig. 9.9. Poincaré maps of the Hénon-Heiles system, for three values of the dimensionless energy $e \equiv E/E_0$, with $E_0 \equiv m_1 \omega_1^2 / \varepsilon^{2/3}$. Adapted from M. Hénon and C. Heiles, *The Astron. J.* **69**, 73 (1964).

However, starting from some value of energy, certain initial conditions lead to series of points scattered over final-area parts of the Poincaré plane – see the top right panel of Fig. 20. This means that the corresponding oscillations $q_2(t)$ do not repeat from one (quasi-) period to the next one – cf. Fig. 4 for the dissipative, forced pendulum. This is chaos.²³ However, some other initial conditions still lead to closed contours. This feature is similar to billiards, and typical for Hamiltonian systems. As the energy is increased, the larger and larger part of the Poincaré plane belongs to the chaotic motion, signifying deeper and deeper chaos.

²² See, e.g., M. V. Berry, in: S. Jorna (ed.), *Topics in Nonlinear Dynamics*, AIP Conf. Proc. No. 46, AIP, 1978, pp. 16-120.

²³ This fact complies with the necessary condition of chaos, discussed in the end of Sec. 2, because Eq. (20) may be rewritten as a system of four differential equations of the first order.

9.4. Chaos and turbulence

This extremely short section consists of essentially one statement. Returning to our discussion of turbulence in Sec. 8.5, I have to note that the (re-)discovery of the deterministic chaos in systems with just a few degrees of freedom in the 1960s considerably changed the tone of debates concerning origins of turbulence. First, the extreme point of view, which paralleled the notions of chaos and turbulence, became leading the debate.²⁴ However, after an initial excitement, significant evidence of the Landau-style mechanisms, involving many degrees of freedom, has been rediscovered and could not be ignored any longer. To the best knowledge of this author (who is a very distant observer of that field), most experimental and numerical-simulation data carry features of both mechanisms, so that the debate continues.²⁵ The reader has more chances to see where will this discussion end eventually (if it will:-).²⁶

²⁴ An important milestone on that way was the work by S. Newhouse, D. Ruelle, and F. Takens, *Comm. Math. Phys.* **64**, 35 (1978), who have proven the existence of a strange attractor in a rather abstract model of fluid flow.

²⁵ See, e.g., U. Frisch, *Turbulence: The Legacy of A. N. Kolmogorov*, Cambridge U. Press, 1996.

²⁶ The reader interested in the deterministic chaos as such may also like to have a look at a very popular book S. H. Strogatz, *Nonlinear Dynamics and Chaos*, Westview, 2001.